Experimental Investigation on the Reliability of Thermal Wave Interferometry in the Thermophysical Characterization of Plasma Sprayed Coatings

A. Bendada,[1,2] **N. Baddour,**[3] **A. Mandelis,**[3] **and C. Moreau**[1]

The main focus of this work is to compare thermal diffusivity and effusivity data resulting from thermal wave interferometry (TWI) experiments on tungsten coatings of different thicknesses with those obtained using reference techniques, namely, the laser flash method and scanning electron microscopy (SEM). The deviations between TWI and the latter techniques are discussed in terms of lack of data in the low frequency range. The investigation shows that the lack of data at low frequencies does not affect diffusivity measurements, while it has a strong effect on effusivity measurements for thermally thick coatings. The conclusions of this experimental study are in good agreement with theoretical predictions resulting from a sensitivity analysis reported in a previous study.

KEY WORDS: coating; plasma-spray; thermal conductivity; thermal diffusivity; thermal effusivity; thermal wave interferometry; tungsten; zirconia.

1. INTRODUCTION

A number of photothermal methods using as the heating source either a modulated laser or a pulsed thermal source have been employed to determine the thickness or the thermal properties of coatings [1–14]. The current paper focuses on the analysis of the accuracy of thermal wave interferometry (TWI) in determining the thermal characteristics of coatings. This is carried out through an experimental comparison analysis

---

[1]National Research Council, Industrial Materials Institute, 75 De Mortagne Boulevard, Boucherville, Quebec J4B 694, Canada.
[2]To whom correspondence should be addressed. E-mail: akim.bendada@cnrc-nrc.gc.ca
[3]Center for Advanced Diffusion-Wave Technologies, University of Toronto, Toronto, Ontario M5S 3G8, Canada.

of TWI with reference techniques applied to tungsten coatings plasma sprayed onto copper substrates. TWI results are compared to thermal diffusivity measured by the flash method [8, 10, 11] and to the heat effusivity estimated from the combination of the thermal diffusivity measured by the flash method and the specific heat of the coating. This one is calculated using the specific heat of tungsten and air, and the air porosity in the coating measured via scanning electron microscopy (SEM). Discrepancies between the techniques are discussed in terms of coating thermal thickness and lack of experimental data at low frequencies. At the end of the description of the investigation on tungsten specimens, for comparison reasons, we give the main results that were obtained in previous work [14] that dealt with plasma sprayed zirconia coatings. Zirconia is a much better thermal insulator than tungsten.

2. DESCRIPTION OF THERMAL WAVE INTERFEROMETRY

2.1. Theory

In the TWI technique, the coating surface is heated periodically and the resulting periodic thermal response at the surface is recorded with a detector, and then processed to obtain the required information on the coating. Among the main features of TWI is that the thermo-signal at the coating surface is out of phase with the heating source. In practice, the experimental surface temperature is normalized by the surface temperature, obtained at the same conditions, of a semi-infinite homogeneous material. The normalizing procedure is necessary to remove system frequency dependences from the experimental data. The expression of the normalized phase shift with respect to the applied periodic heating, which was first obtained by Benett and Patty [4] in 1982, is given by

$$\varphi = -\tan^{-1}\left[\frac{2R\exp(-x)\sin(x)}{1 - R^2\exp(-2x)}\right] \tag{1}$$

in which $x = 2L/\mu$, L is the coating thickness, μ is the thermal diffusion length $\mu = [\alpha_c/(\pi f)]^{1/2}$, α_c is the normal thermal diffusivity, and f is the frequency. R is the thermal wave reflection coefficient defined as $R = (1 - b)/(1 + b)$, and $b = [(\rho C_p k)_s/(\rho C_p k)_c]^{1/2}$ gives the ratio of the substrate and coating thermal effusivities e_s and e_c.

Equation (1) shows that the governing thermal quantities for the phase shift changes with frequency are the reflection coefficient R and the characteristic thermal diffusion time $t_c = L^2/\alpha_c$. A nonlinear least-squares fit of phase vs. frequency measurements can then be used to identify these two quantities. The coating thermal diffusivity is obtained from

the characteristic thermal diffusion time if the coating thickness is known, and the coating thermal effusivity is obtained from the reflection coefficient if the substrate effusivity is known.

2.2. Sensitivity of Thermal Wave Interferometry

In order to check the uniqueness and the reliability of the solution, some issues have to be considered. One of them is the influence of the measurement noise on the unknowns. Another is the amount of experimental data available. This has already been dealt with in a previous study [14] after a detailed examination of the sensitivity coefficients. Let us recall that only two sensitivity coefficients are involved in the current investigation. They are defined as the first derivative of the phase shift with respect to the unknown parameters, namely, the thermal diffusivity and effusivity. Sensitivity theory stipulates that if the sensitivity coefficients are either small or correlated with one another, the estimation problem is difficult and very sensitive to measurement noise [15, 16]. In other words, the best way to make an inversion problem effective is to use only experimental data in the regions where the sensitivity coefficients are high, not proportional, nor almost proportional, nor, in general, constitute a linear combination. If for any reason, such as an experimental setup limitation, for example, the experimental data are available only in the regions where the unknown parameters have a negligible or a correlated effect on the phase signal, the use of those data may lead to huge errors in the solutions. The reader may refer to Ref. 14 for details and main conclusions of the theoretical sensitivity analysis.

3. EXPERIMENTAL PROCEDURE

3.1. Description of the Samples

Four samples were produced by plasma-spraying tungsten coatings onto a 10-mm-thick copper substrate. The coatings (123, 223, 449, 835 μm thickness) were obtained with commercial tungsten powder of particle size distribution varying from 5.6 to 45 μm (H.C. Starck, Amperit 140.3). The powder spray rate was adjusted to get a deposition rate of 12 μm/pass. The carrying argon gas flow was set at 7 L·min^{-1}. The plasma-spraying torch was laterally scanned at 0.6 m·s^{-1}. The torch was a Plasmadyne SP-100 with a No. 129 cathode, No. 145 anode, and No. 130 gas injector. The power was 28 KW (800 A and 35 V). The arc gas was argon, and the auxiliary gas was helium (32% helium, with 50 L·min^{-1} for argon and 24 L·min^{-1} for helium). The standoff distance during spraying was

76 mm. The substrate was cooled with a nitrogen jet, while the front sur-
face was air-blasted to eliminate aerosols.

3.2. Characterization Using Thermal Wave Interferometry

To validate the sensitivity conclusions described in Ref. 14 and to
investigate the reliability of TWI, we carried out TWI experiments on
the plasma-sprayed tungsten coatings. The experimental system for sam-
ple frequency scans is shown in Fig. 1. A high power 20-W laser
(Jenoptik JOLD-X-CPXL-1L) was current-modulated using a Thorlabs
high power laser driver with a maximum modulation-frequency capability
of 10 kHz and minimum frequency capability of 0.1 Hz. The largely aniso-
tropic multi-mode laser beam was expanded, collimated, and then directed
onto the surface of the sample. The infrared (Planck) radiation from the
optically excited sample surface was collected and collimated by two sil-
ver-coated, off-axis paraboloidal mirrors and then focused onto a liquid-
nitrogen-cooled HgCdTe (mercury–cadmium–telluride) detector (EG&G
Judson Model J15016-M204-S01M-WE-60). The heated area of the sam-
ple was at the focal point of the mirror positioned near the sample, and
the detector was at the focal point of the other mirror. The HgCdTe detec-
tor is a photoconductive element that undergoes a change in resistance
proportional to the intensity of the incident infrared radiation. Our detec-
tor had an active square-size area of 1×1 mm and a spectral bandwidth
of $2 - 12 \,\mu$m. An anti-reflection coated germanium window with a trans-
mission bandwidth of $2 - 14 \,\mu$m was mounted in front of the detector
to block any radiation from the laser. Prior to being sent to the dig-
ital lock-in amplifier (EG&G Instruments Model 7265), the photother-
mal radiometric (PTR) signal was amplified by a low-noise pre-amplifier
(EG&G Judson PA101), specially designed for operation with the HgCdTe
detector. The lock-in amplifier, which was interfaced with a PC, received
and demodulated the pre-amplifier output (thermal-wave amplitude and
phase). The process of data acquisition, storage, and frequency scanning
was fully automated.

Frequency scans from 0.1 to 200 Hz were performed with a large laser
beam size (> 1.5 cm) to keep the photothermal response one-dimensional.
System transfer-function normalization was achieved by performing the
same one-dimensional experiment with a homogeneous (untreated) sam-
ple, a Zr alloy, and using this frequency scan to normalize the frequency
scans of the coated samples. Normalization problems due to the inade-
quacy of our reference sample were observed in the data below approxi-
mately 0.3 Hz. Calculations of the thermal diffusion length showed that for
very low frequencies, the thermal diffusion length of zirconium was longer
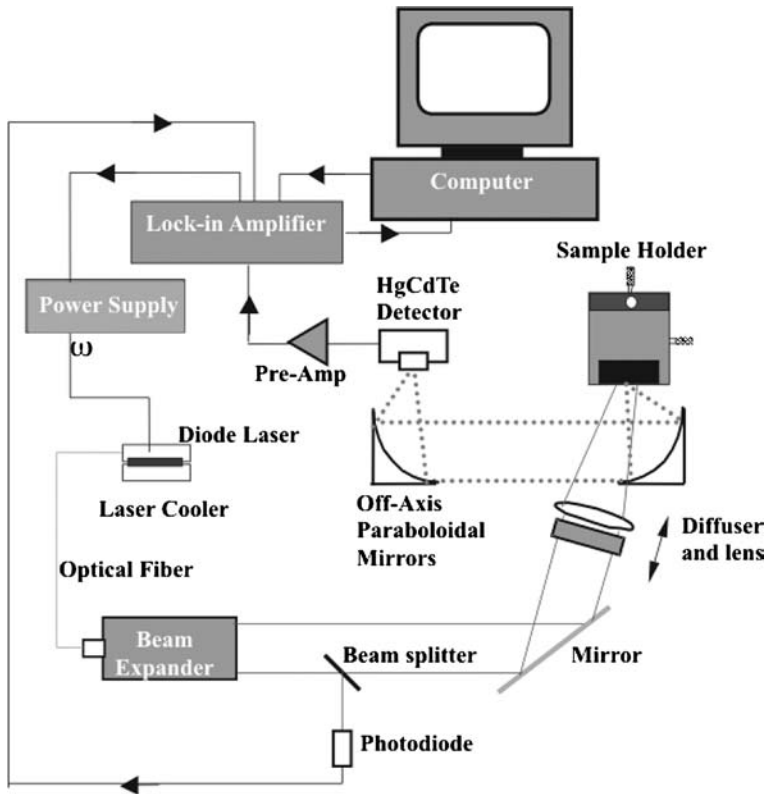
Fig. 1. Schematic representation of the thermal wave interferometry testing system.

than the thickness of the sample itself. For this reason, the first 10 points of the normalized data have been set aside as ignored data. These data can be used as long as we normalize the points by a proper semi-infinite reference sample. In the unnormalized form, they have relative value and can also be used to observe signal trends.

The normalized phase data above ~0.3 Hz have been plotted in Fig. 2. The magnitude of the phase vs. frequency curves reported in Fig. 2 suggests a reflection coefficient R to be around -0.90. As stated in the conclusions resulting from the sensitivity analysis for large R-values, this case is very suitable for accurate diffusivity estimation [14]. The effusivity should also be accurately estimated because it still has quite a high sensitivity at a thin thermal thickness. However, since useful experimental phase data were not available for frequencies below 0.3 Hz, we did not expect to obtain precise estimations of effusivity for thermally thick coatings
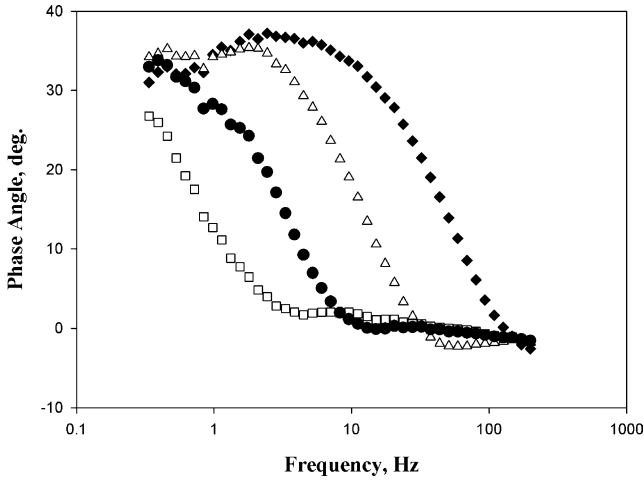
Fig. 2. Normalized phase versus frequency curves of copper substrate with tungsten coating of thickness 123 (■), 223 (△), 449 (●), and 835 μm (□).

($L = 449$ and $835\,\mu$m). The reason is that, for high R-values, the sensitivity to the effusivity reaches an extremum at very low thermal thicknesses, and then changes rapidly to weak values at larger thermal thicknesses [14]. On the other hand, diffusivity measurements were still expected to be quite accurate. Indeed, the maximum sensitivity to diffusivity is within the decreasing part of the phase vs. frequency curve, and the lack of data at low frequencies did not have a serious impact on its estimation. Figure 3 shows a typical example of the nonlinear numerical fit of the experimental data with Eq. (1) for the 123-μm-thick sample. The substrate effusivity, which was needed in the TWI technique to extract the coating effusivity from the estimated reflection coefficient, was determined by combining the diffusivity measured by the laser flash method and the specific heat measured by modulated differential scanning calorimetry (MDSC); $e_s = 57606\,\mathrm{J \cdot m^{-2} \cdot {}^\circ C^{-1} \cdot s^{-1/2}}$. Table I summarizes the results obtained from all the samples analyzed by the TWI technique. We also mention for reference that because of the low level of the roughness compared to the coating thickness, effects of roughness were neglected in the frequency range (0.3 – 200 Hz) used during the processing of the phase data. This assumption is based on the fact that for low roughness levels, the phase signal is affected by roughness only at very high frequencies and less influenced at low frequencies where it exhibits the behavior of a homogeneous coating [17].
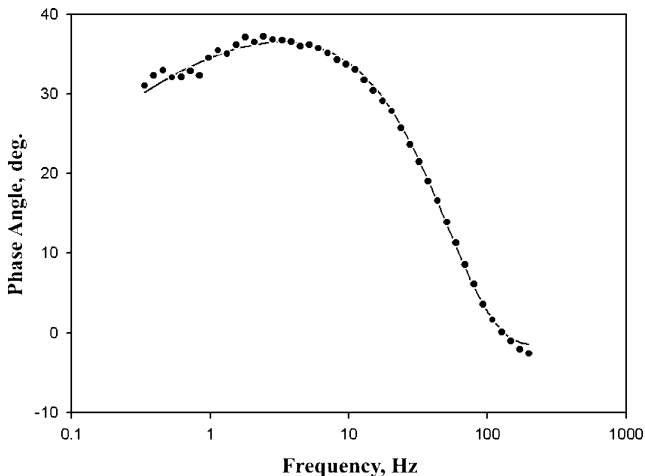
Fig. 3. Numerical fitting of the thermal diffusivity and effusivity for the thinner tungsten coating (thickness $L = 123\,\mu$m).

Table I. Diffusivity and Effusivity of Tungsten Coating Obtained by TWI

Sample no.	L (μm)	$\alpha(10^{-6}\,\mathrm{m^2 \cdot s^{-1}})$	R	e (J·m^{-2}·°C^{-1}·s$^{-1/2}$)
1	123 ± 14	2.24 ± 0.36	-0.897 ± 0.008	3135 ± 160
2	223 ± 22	3.40 ± 0.48	-0.879 ± 0.016	3691 ± 325
3	449 ± 11	4.70 ± 0.47	-0.808 ± 0.057	6132 ± 1252
4	835 ± 19	5.24 ± 0.37	-0.681 ± 0.082	10931 ± 2083

3.3. Validation Using Laser Flash and Scanning Electron Microscopy Methods

To validate the thermal diffusivity and effusivity measured by TWI, we performed comparison measurements using the laser flash and SEM experiments. The latter techniques are considered very reliable and highly accurate and can thus be used as reference techniques for the validation of TWI. To carry out the laser flash and SEM techniques, it was necessary to separate the coatings from the substrates. This was done by chemical etching for 2 h in a 50% water solution of nitric acid, which did not substantially attack tungsten. In this experiment, we projected a YAG laser pulse, of nearly 600 μs duration and 10 J energy, over the full front face of the sample so that the heat transfer could be considered as one-dimensional. The temperature evolution with time at the center of
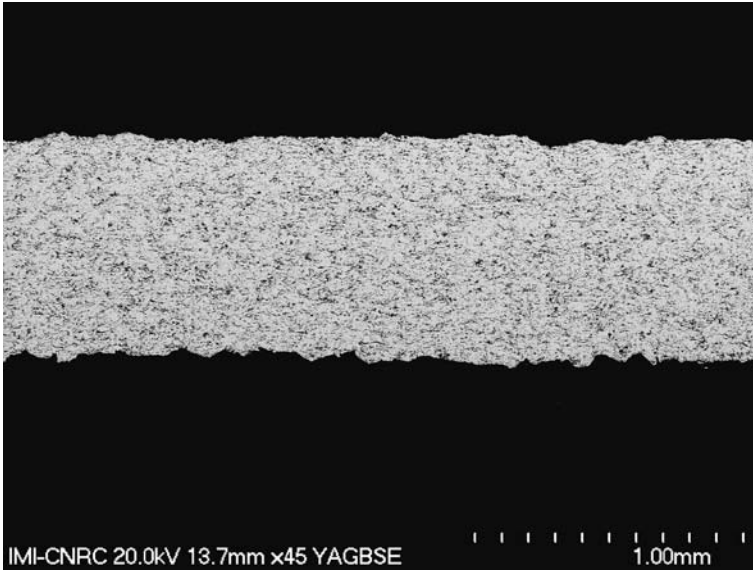
Fig. 4. Typical image obtained via scanning electron microscopy of the cross section of the 835-μm-thick tungsten coating.

the back face was monitored by an InSb infrared detector. The temperature data were first processed to determine the characteristic time $t_c = L^2/\alpha_c$. To estimate the diffusivity from the latter characteristic time, the coating thickness L was subsequently measured using the coating cross-section images provided by SEM. Figure 4 shows a typical microscopic image obtained from the 835-μm-thick tungsten coating. Measured coating thicknesses with their standard deviations are reported in Tables I–IV. Thermal diffusivities measured by the laser flash method are reported in Table II. Knowing the diffusivity α_c measured by the laser flash method, it was possible to evaluate the effusivity of the coating using the following relationship: $e_c = (\rho C_p)_c (\alpha_c)^{1/2}$. The specific heat of the coating $(\rho C_p)_c$ is simply given by $(\rho C_p)_c = (\rho C_p)_{air} F + (\rho C_p)_w (1 - F)$, where F is the coating porosity, and $(\rho C_p)_{air}$ and $(\rho C_p)_w$ are the specific heats of air and tungsten, respectively. The coating porosity F was determined from the processing of the images obtained from SEM taken at $500\times$ in the backscatter mode. For each coating, the porosity was calculated from 10 images randomly selected on the coating cross section. The estimated thermal effusivities and uncertainties are reported in Table III.

In a previous investigation [14], we used the same strategy to analyze the accuracy of TWI in characterizing the thermal properties of a

Table II. Diffusivity of Tungsten Coating Obtained by the Laser Flash Method

Sample no.	$L(\mu\text{m})$	$\alpha(10^{-6}\,\text{m}^2\cdot\text{s}^{-1})$
1	123 ± 14	2.32 ± 0.25
2	223 ± 22	3.22 ± 0.33
3	449 ± 11	4.39 ± 0.27
4	835 ± 19	5.51 ± 0.34

Table III. Effusivity of Tungsten Coating Obtained by the Combination of the Diffusivity Measured by the Laser Flash Method and the Specific Heat Calculated Using the Coating Porosity Measured with SEM, as well as the Specific Heats of Tungsten and Air

Sample no.	$L\,(\mu\text{m})$	$\alpha\,(10^{-6}\,\text{m}^2\cdot\text{s}^{-1})$	$F\,(\%)$	$\rho C_\text{p}(10^6\,\text{J}\cdot\text{m}^{-3}\cdot{}^\circ\text{C}^{-1})$	$e\,(\text{J}\cdot\text{m}^{-2}\cdot{}^\circ\text{C}^{-1}\cdot\text{s}^{-1/2})$
1	123 ± 14	2.32 ± 0.25	16.4 ± 1.4	2.17 ± 0.04	3244 ± 60
2	223 ± 22	3.22 ± 0.33	15.7 ± 1.3	2.19 ± 0.03	4030 ± 55
3	449 ± 11	4.39 ± 0.27	10.5 ± 3.1	2.32 ± 0.08	5029 ± 173
4	835 ± 19	5.51 ± 0.34	15.7 ± 1.8	2.19 ± 0.05	5004 ± 114

plasma-sprayed zirconia coating. We will recall for reference only important results of the study. The reader may refer to the above-mentioned article for a detailed description. Compared to tungsten, zirconia has a lower thermal diffusivity (5 – 8 times lower). On the other hand, the thinnest zirconia coating that was investigated had a thickness of $252\,\mu\text{m}$. As a consequence, the investigated zirconia coatings had a much higher thermal thickness than the tungsten specimens described in the current work. Moreover, the TWI setup that was employed at that time to test the zirconia specimens was limited by the lock-in amplifier frequency range to frequencies higher than $0.5\,\text{Hz}$. All these factors caused the TWI measurements to be restricted only to the decreasing part of the phase signal as shown in Fig. 5. This figure reports the experimental data for the three zirconia coatings, $L = 252$, 317, and $494\,\mu\text{m}$. As predicted by the sensitivity analysis, because of the lack of data at low frequencies, we did not obtain precise estimations for the effusivity. However, diffusivity measurements were quite accurate. Table IV summarizes the discrepancies between the thermal properties provided by the TWI technique and those given by the laser flash and MDSC measurements for the zirconia specimens.
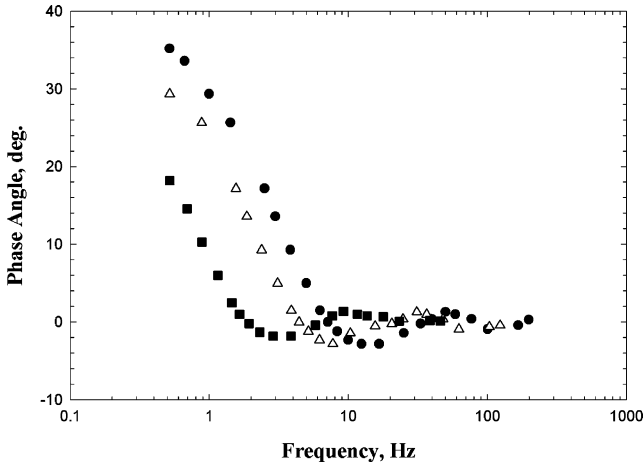
Fig. 5. Normalized phase vs. frequency curves of copper substrate with zirconia coating of thickness 252 (●), 317 (△), and 494 μm (■).

Table IV. Discrepancies of TWI with Respect to the Laser Flash and MDSC Measurements for Zirconia Coatings

Sample no.	L (μm)	$\Delta\alpha/\alpha$ (%)	$\Delta e/e$ (%)
1	252 ± 27	+6.95	+24.31
2	317 ± 21	+3.16	−14.32
3	494 ± 12	−3.93	−71.57

3.4. Discussion

It can be seen from Tables I–III that TWI provides diffusivity values comparable to those obtained with the laser flash method. Table V summarizes the relative deviations between the thermal properties provided by the TWI technique and those given by the laser flash and SEM measurements. The diffusivity errors were less than 7%, which is comparable to the standard precision of the laser flash method, 5%. With regard to effusivity, the agreement was acceptable only for the thin tungsten coatings ($L = 123$ and $223\,\mu$m), where the absolute relative discrepancy did not exceed 8.43%. For the thicker coatings, the discrepancy in effusivity measurements was quite high, more than 21% for the 449-μm-thick coating and more than 118% for the 835-μm-thick coating. This confirms the conclusions of the sensitivity analysis for the determination of the effusivity in the case

Table V. Discrepancies of TWI with Respect to the Laser Flash and SEM Measurements for Tungsten Coatings

Sample no.	L (μm)	$\Delta\alpha/\alpha$ (%)	$\Delta e/e$ (%)
1	123 ± 14	$+3.43$	-3.38
2	223 ± 22	-5.67	-8.43
3	449 ± 11	-7.03	$+21.92$
4	835 ± 19	$+4.81$	$+118.43$

of thermally thick coatings when the experimental design provides useful data only in the high-frequency range. In the experimental apparatus used in this work, the useful frequency range was limited to frequencies larger than 0.3 Hz.

With regard to the zirconia coatings, it can be seen clearly from Table IV that the measurement of diffusivity by TWI is quite acceptable. The diffusivity errors were less than 7%. On the other hand, the absolute effusivity error was in the range 14 – 71%. These percentage errors are not comparable to standard effusivity evaluation techniques (uncertainty < 5%) and are too large to be acceptable. However, it should be pointed out here that these results for zirconia coatings were obtained in unfavorable evaluation conditions: large coating thickness and low thermal diffusivity.

We also mention for reference that the thermal properties of the coatings, determined by both techniques and shown in Tables I – III, appear to be significantly correlated with their thickness. The reader should be aware that this feature is not related to the techniques used for the characterization but is caused by differences in coating microstructure. The latter differences are due to the increase in the coating temperature during spraying: Thicker coatings heat up to higher temperatures during spraying, resulting in a lower particle-to-particle thermal contact resistance.

4. CONCLUSION

This work has dealt with the analysis of the accuracy of TWI in estimating the thermal properties of coatings. First, we characterized four plasma-sprayed tungsten coatings, each with a different thickness. Then, we compared the TWI results with those obtained using the laser flash method and SEM. The discrepancies were discussed in terms of lack of useful data in the low frequency range, below 0.3 Hz. Indeed, the ref-

erence sample used for instrumental transfer-function normalization during the TWI experiments did not provide useful phase data in the latter frequency range. The study has shown that the lack of data at low frequencies did not affect diffusivity measurements. However, it had a strong effect on the characterization of the effusivity of thermally thick coatings. The experimental results confirmed the conclusions obtained by a theoretical sensitivity study that has previously been performed [14] to determine the critical parameters that influence the accuracy of TWI.

ACKNOWLEDGMENTS

REFERENCES

1. D. Almond and P. Patel, *Photothermal Science and Techniques* (Chapman & Hall, London, 1996).
2. J. A. Garcia, A. Mandelis, B. Farajbakhsh, C. Lebowitz, and I. Harris, *Int. J. Thermophys.* **20**:1587 (1999).
3. C. Moreau, P. Fargier-Richard, R. G. Saint-Jacques, and P. Cielo, *Surf. Coat. Tech.* **61**:67 (1993).
4. C. A. Benett Jr. and R. R. Patty, *Appl. Opt.* **21**:49 (1982).
5. D. P. Almond, P. M. Patel, and H. Reiter, *Mater. Eval.* **45**:471 (1987).
6. S. K. Lau, D. P. Almond, and P. M. Patel, *J. Phys. D: Appl. Phys.* **24**: 428 (1991).
7. J. D. Morris, D. P. Almond, P. M. Patel, and H. Reiter, in *Photoacoustic and Photothermal Phenomena 2*, J. C. Murphy, J. W. Maclachlan Spicer, L. Aamodt, and B. S. H Royce, eds. (Springer Verlag, Berlin, 1990), pp. 71–73.
8. R. E. Taylor, *Mater. Sci. Eng.* **A245**:160 (1998).
9. D. P. Almond, P. M. Patel, I. M. Pickup, and H. Reiter, *NDT Int.* **18**:17 (1985).
10. P. Cielo and S. Dallaire, *J. Mater. Eng.* **9**:71 (1987).
11. A. S. Houlbert, P. Cielo, C. Moreau, and M. Lamontagne, *Int. J. Thermophys.* **15**:525 (1994).
12. B. K. Bein, J. Bolte, D. Dietzel, A. Haj Daoud, G. Kalus, F. Macedo, A. Linnenbrugger, H. Bosse, and J. Pelzl, *Surf. Coat. Tech.* **116–119**:147 (1999).
13. A. C. Bento, D. P. Almond, S. R. Brown, and I. G. Turner, *J. Appl. Phys.* **79**:6848 (1996).
14. A. Bendada, M. Lamontagne, and H. Roberge, *Int. J. Thermophys.* **24**:207 (2003).
15. J. V. Beck, and K. J. Arnold, *Parameter Estimation in Engineering and Science* (Wiley, New York, 1977).
16. X. Maldague, A. Bendada, M. Bertolotti, G. L. Liakhou, R. Li Voti, S. Paoloni, Y. A. Plotnikov, and C. Cibilia, in *Nondestructive Testing Handbook, vol. 3: Infrared and Thermal Testing* (American Society for Nondestructive Testing, 2001), pp. 273–385.
17. L. Nicolaides and A. Mandelis, *J. Appl. Phys.* **90**:1255 (2001).